

Quantum Dots

How to cite:

International Edition: doi.org/10.1002/anie.202202322

German Edition: doi.org/10.1002/ange.202202322

Minimizing the Reorganization Energy of Cobalt Redox Mediators Maximizes Charge Transfer Rates from Quantum Dots

Madeleine J. Fort, Sophia M. Click, Evan H. Robinson, Felix M. C. He, Paul V. Bernhardt, Sandra J. Rosenthal, and Janet E. Macdonald*

Abstract: Light-induced charge separation is at the very heart of many solar harvesting technologies. The reduction of energetic barriers to charge separation and transfer increases the rate of separation and the overall efficiency of these technologies. Here we report that the internal reorganization energy of the redox acceptor, the movement of the atoms with changing charge, has a profound effect on the charge transfer rates from donor quantum dots. We experimentally studied and modelled with Marcus Theory charge transfer to cobalt complexes that have similar redox potentials covering 350 mV, but vastly different reorganization energies spanning 2 eV. While the driving force does influence the electron transfer rates, the reorganization energies had a far more profound effect, increasing charge transfer rates by several orders of magnitude. Our studies suggest that careful design of redox mediators to minimize reorganization energy is an untapped route to drastically increase the efficiency of quantum dot applications that feature charge transfer.

Introduction

Quantum confined semiconductor nanocrystals, also known as quantum dots (QDs), are widely used in photovoltaics, hydrogen generation, light emission, and probes for biological samples.^[1–5] Their highly tunable band gaps, large Stokes shift, greater ability for surface functionalization, and high degree of photostability make quantum dots ideal subjects for experimentation.^[6–8] QDs are ubiquitous across many fields of study, however, there are still many fundamental questions about their behavior which have yet to be answered.

Many applications of QDs require the separation and extraction of charge.^[9] Increasing the rate of charge transfer is key to improving the efficiency and sensitivity of several of the aforementioned applications. QD fluorescence quenching in the presence of an electron acceptor is an indirect way to observe charge transfer kinetics. While observing a change in fluorescence intensity of the QDs is almost trivial, the determination of what mode caused that change and what factors contributed is challenging.^[10,11] Not only are there a large number of possible charge and energy transfer pathways, including non-radiative recombination, radiative energy transfer, charge transfer, and radiative recombination, but there is significant evidence that, due to the intermediate density of states between that of the bulk and a molecule, hole and electron transfer from quantum dots does not necessarily follow bulk transfer or molecular transfer models.^[12,13]

For nanocrystals, molecular charge transfer models are often applied despite limitations. In molecular charge transfer, the Marcus Electron Transfer Theory has been shown to describe the relationship between driving force and transfer rates.^[14] The high accuracy of the predictions is, in large part, due to the inclusion of the reorganization energy (λ) to the model. Reorganization energy is the shift in nuclear coordinates upon the transfer of charge and includes (inner sphere) vibrational shifts (such as changing bond lengths) in both the donor and acceptor species as well as (outer sphere) movements in the surrounding solvent.^[15]

In the Marcus model, there are three regions dictated by the relationship between driving force (ΔG) and reorganization energy. Where $-\Delta G < \lambda$, the system is in the normal region and an increase in driving force leads to higher charge transfer rates. Where $-\Delta G \approx \lambda$, the system is at the peak transfer rate, called the barrierless region. Lastly, when $-\Delta G > \lambda$, the system is in the inverted region and further increases in driving force should lower the transfer rate. With this heavy dependence of transfer rates on the relationship of the reorganization energy to driving force, it is odd that so little attention has been given to using reduced reorganization energy to improve charge transfer rates from quantum dots and in other photoelectrochemical systems. Understanding the precise nature of this relationship for electron transfer (ET) mechanisms can lead to greater efficiencies in solution redox mediated processes, especially in dye and quantum dot-sensitized solar cells, and photoelectrochemical water splitting.

Chelated cobalt complexes as acceptors provide an opportunity to examine charge transfer from quantum dots

[*] M. J. Fort, S. M. Click, Dr. E. H. Robinson, Dr. S. J. Rosenthal, Dr. J. E. Macdonald
Department of Chemistry,
Vanderbilt Institute of Nanoscale Science and Engineering
Vanderbilt University
Nashville, TN 37235 (USA)
E-mail: janet.macdonald@vanderbilt.edu
Dr. F. M. C. He, Dr. P. V. Bernhardt
School of Chemistry and Molecular Biosciences
University of Queensland
Brisbane, Queensland,
4072 (Australia)

in a technologically relevant way. Cobalt complexes have been studied as efficient redox mediators for a variety of charge transfer applications including protein electron transfer, Dye Sensitized Solar Cells (DSSCs), and H₂ generation.^[16–22]

In one example, a tethered cobalt complex accepted photogenerated electrons from CdTe QDs on the picosecond timescale, and also acted as an active catalyst center for reducing water to H₂.^[23]

In dye-sensitized solar cells, cobalt complexes are less corrosive redox mediators than the traditional tri-iodide/iodide couple and the electrochemical potentials are better placed energetically to provide a larger open circuit voltage in the device.^[24] Cobalt complexes were used with porphyrin sensitized solar cells to produce an efficiency of 12% and outperformed the iodide couple.^[25] Various attempts have been made to improve upon the 12% efficiency, and researchers have identified high reorganization energies of the dyes and the cobalt redox complexes as limiting factors.^[17,26–28] It is thought that a large component of this high reorganization energy comes from the transition from low-spin Co^{III} to high-spin Co^{II} prompting the search for and use of complexes which do not undergo this transition.^[26] Here, we demonstrate the power of carefully designed ligand cage environments around the cobalt center to minimize reorganization energy, and increase charge transfer rates by several orders of magnitude.

In this work, cadmium chalcogenide quantum dots were used as charge donors because their optical properties are well studied. Since they are much larger than a molecule, the reorganization energy of QDs can be assumed to be negligible, allowing the influence of the reorganization of the acceptor to be isolated.^[29] While it would seem that Marcus theory would already dictate the precise effect, many studies ignore or simply estimate the internal reorganization energy of the charge acceptor. Often, only the reorganization energy due to the solvent is considered significant when calculating the transfer rates. Studies have shown that solvent reorganization energy of molecular acceptors can be modestly manipulated by using less polar solvents to improve charge transfer, yet many applications will dictate that aqueous conditions be used.^[30] For this reason, we chose to only study aqueous conditions here.

Internal reorganization of a charge acceptor can be very consequential, and even larger than the solvent reorganization energy. It is unexplored whether minimization of the internal (inner sphere) reorganization energy can be employed as an effective strategy to improve function in applications that require charge transfer from quantum dots.

Here we study photoinduced charge transfer from QDs to three cobalt complex ions: tris(ethylenediamine)cobalt(III/II) abbreviated as [Co(en)₃]^{3/2+} (1), and the caged complexes (sepulchrate)cobalt(III/II) abbreviated as [Co(sep)]^{3/2+} (2), and (1-chloro-8-methyl-3,13,16-trithia-6,10,19-triazabicyclo[6.6.6]icosane)cobalt(III/II) abbreviated as [Co(ClMeN₃S₃sar)]^{3/2+} (3) (Figure 1, Table 1).^[16,35] These three cobalt complexes were chosen because they have similar electrochemical reduction potentials that are within 350 mV, but have very different reorganization energies spanning

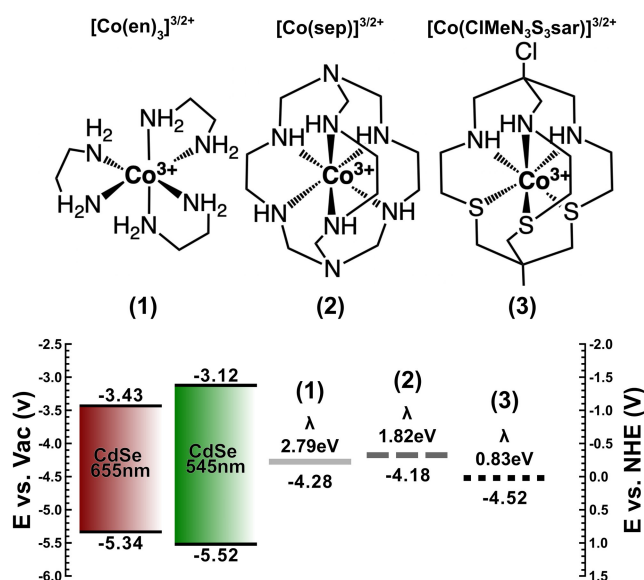


Figure 1. Internal reorganization energies and reduction potentials of the studied cobalt complexes and estimated band positions for idealized CdSe QDs.

Table 1: Properties of cobalt redox mediators.

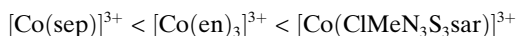
	$K_{AA}M^{-1}s^{-1}$	λ_i [eV] ^[b]	E° (V) ^[c]
[Co(en) ₃] ^{3/2+}	2.0×10^{-5} ^[a]	2.79 [3.24]	-0.224
[Co(sep)] ^{3/2+}	5.1 ^[b]	1.82 [2.28]	-0.323
[Co(ClMeN ₃ S ₃ sar)] ^{3/2+}	10^4 ^[c]	0.83 [1.27]	0.022

K_{AA} is the self-exchange rate constant of the cobalt complexes from [a] Reference [31], [b] Reference [32,33], [c] Reference [34]. λ_i is the calculated internal reorganization energy. λ includes the solvent (aqueous) reorganization energy which was estimated to be 0.45 eV. E° is the reduction potential (vs NHE) measured through cyclic voltammetry (Supporting Information).

nearly 2 eV. These structurally similar amine-chelated complexes are also less prone to ligand exchange than monodentate ligated complexes. Marcus theory is employed to predict the electron transfer rates from green and red fluorescent cadmium chalcogenide quantum dots, to include both effects of reorganization energy and driving force. The predicted trends are shown experimentally through steady-state and time-resolved photoluminescence. The results highlight the dominant role of the complexes' different reorganization energies on altering the charge transfer rates by 3–4 orders of magnitude, over the role of driving force. The experimental results suggest that Auger-Assisted charge transfer, is potentially an active charge transfer mechanism that is not commonly included in Marcus predictions.

Results and Discussion

The electrochemical properties and the reduction potentials of the three $\text{Co}^{3/2+}$ complexes were measured by cyclic voltammetry (Table 1). When plotted against the approximate band edges of red and green fluorescing CdSe QDs, the reduction potentials of the three cobalt complexes, $[\text{Co}(\text{ClMeN}_3\text{S}_3\text{sar})]^{3/2+}$, $[\text{Co}(\text{en})_3]^{3/2+}$ and $[\text{Co}(\text{sep})]^{3/2+}$ sit within the band gap of the QDs (Figure 1) and span about 350 mV. The driving force for electron transfer from the conduction band of a QD to one of these complexes therefore follows as:



The trend is reversed for the driving force for hole transfers from the QD valence band to Co^{2+} ions.

The three chosen cobalt complexes have massively different reported self-exchange rates covering nine orders of magnitude (Table 1). The more rigid cage structure of $[\text{Co}(\text{sep})]^{3/2+}$ limits movement of the ligand shell and has a much faster self-exchange rate ($5.1 \text{ M}^{-1} \text{ s}^{-1}$) than $[\text{Co}(\text{en})_3]^{3/2+}$ ($2.0 \times 10^{-5} \text{ M}^{-1} \text{ s}^{-1}$). While most Co^{II} hexamine complexes are high spin, the Co^{II} and Co^{III} forms of $[\text{Co}(\text{ClMeN}_3\text{S}_3\text{sar})]^{3/2+}$ are both low spin, which further limits the demand for structural changes in the ligand sphere upon changing oxidation state. The self-exchange rate constant for $[\text{Co}(\text{ClMeN}_3\text{S}_3\text{sar})]^{3/2+}$ has not been reported but the rate constant for the closely related N-capped analog (where N– replaces C–Cl) has been determined to fall in the range 4.5×10^3 to $2.2 \times 10^4 \text{ M}^{-1} \text{ s}^{-1}$.^[28,36]

The reorganization energies of the three $\text{Co}^{3/2+}$ complexes were estimated from their previously reported self-exchange rates k_f (Table 1). Based on the Marcus Microscopic Model:

$$k_f = K_{P,O} \nu_n \kappa_{el} \exp(-\Delta G_f / RT) \quad (1)$$

Where ΔG_f is the activation energy for the reduction of species O , $K_{P,O}$ is the equilibrium constant between precursor P and species O (which we assume here to be 1), ν_n is the nuclear frequency factor (s^{-1}), and κ_{el} is the electronic transmission coefficient. To calculate the reorganization energy, several assumptions were made; κ_{el} is considered adiabatic and to be unity as the reacting species are close together and there is strong coupling. ν_n is assumed to be $10^{11} \text{ M}^{-1} \text{ s}^{-1}$.^[37] Taking this into account, we can solve for ΔG_f , and further approximate a relationship to the reorganization energy (λ):

$$\Delta G_f = -RT \log(k_f / \nu_n) \approx \frac{\lambda}{4} \quad (2)$$

The reorganization energy is made of both the inner sphere reorganization of the bonds of the molecule, λ_i , and the surrounding solvent, λ_s .

$$(\lambda = \lambda_i + \lambda_s) \quad (3)$$

The solvent reorganization energy was approximated to be 0.45 eV consistent with previous literature^[38] to give approximate internal reorganization energies (Table 1). Solvent reorganization energy can be calculated according to:

$$\lambda_s = \frac{\Delta q^2}{4\pi\epsilon_0} \left(\frac{1}{n^2} - \frac{1}{\epsilon} \right) \left(\frac{1}{d_D} + \frac{1}{d_A} - \frac{2}{R} \right) \quad (4)$$

In this expression, Δq is the change in overall charge, in this case the charge of one electron, n is the refractive index of the solvent, 1.333 for water, ϵ is the dielectric constant, 78.4 for water at 25 °C, d_D is the diameter of the donor, d_A is the diameter of the acceptor and R is the distance over which electron transfer occurs. The second bracketed term is essentially the thickness of the solvent layer between the donor and acceptor. Moving forward we assume that this thickness is approximately the same during self-exchange as with exchange between QDs and the cobalt complexes.

The nine orders of magnitude variation in self-exchange rate for the three complexes equates to a variation in internal reorganization energy spanning approximately two electron volts. While $[\text{Co}(\text{en})_3]^{3/2+}$ was calculated to have an internal reorganization energy of 2.79 eV, the internal reorganization energy for caged $[\text{Co}(\text{sep})]^{3/2+}$ was 1.82 eV and even smaller for the mixed donor cage $[\text{Co}(\text{ClMeN}_3\text{S}_3\text{sar})]^{3/2+}$ at 0.83 eV. The above method of calculating reorganization energy and values given the self-exchange rates gives results that are in good agreement with literature.^[38] It can be imagined that the internal reorganization energy is caused by the expansion and contraction of the ligand environment upon changing the d -orbital occupancy of the cobalt center.

With these reorganization energies and driving forces (ΔG) now in hand, the rates of photoinduced electron transfer from the quantum dots to the cobalt complexes were predicted using the Marcus model (Figure 2).

$$k'_{ET} = \frac{2\pi}{\hbar} \frac{1}{\sqrt{4\pi\lambda k_B T}} \exp \left[-\frac{(\lambda + \Delta G)^2}{4\lambda k_B T} \right] \quad (5)$$

This simplified version includes two important assumptions that preclude direct quantitative comparison with the experiments that follow; the barrier for tunnelling and the electronic coupling (H_{DA}) is assumed to be similar for all three of the complexes to each of the QDs. Variations in shelling between batches of QDs cause these factors to differ from the assumptions due to differences in barrier height. While additional scaling from these factors is likely, much can be learned from the modeled trends, and from experimental comparison within single batches of dots.

In the Marcus model, the reorganization energy presents a barrier to electron transfer, causing the rate of ET to increase with driving force. A remarkable aspect of the model is that when the driving force exceeds the reorganization energy, the rate should decrease in what is known as the Marcus inverted region. This behavior is not always seen in quantum dots, likely due to Auger-Assisted electron transfer.^[12,39]

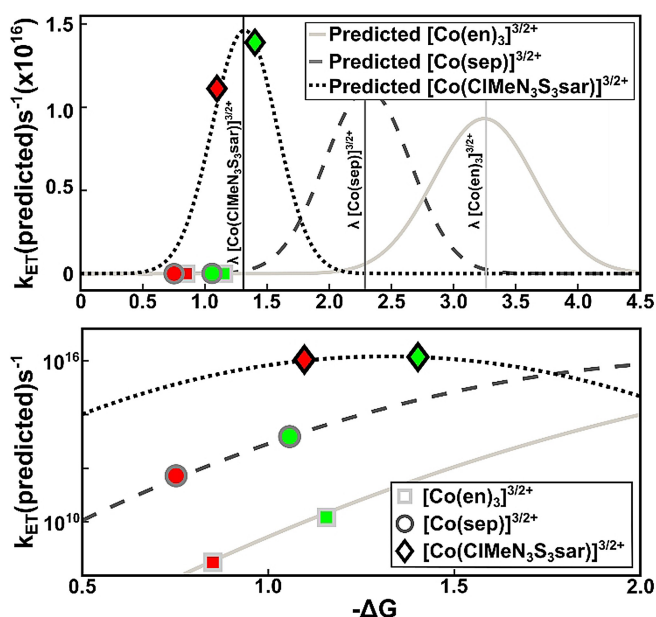


Figure 2. Predictions of the electron transfer rates against driving force according to standard Marcus ET theory for each of the cobalt complexes (lines) and with the specific green and red emitting cadmium chalcogenide QDs employed (colored markers). The bottom graph is on a log scale for clarity.

The prediction is that the electron transfer rates from the conduction band of QDs to $[\text{Co}(\text{ClMeN}_3\text{S}_3\text{sar})]^{3/2+}$ should vastly outstrip the rates for $[\text{Co}(\text{sep})]^{3/2+}$ and $[\text{Co}(\text{en})_3]^{3/2+}$ by at least two orders of magnitude when the driving force is smaller (red QDs) and up to six orders of

magnitude when the driving force is larger (green QDs). While charge transfer from the conduction band of green and red emitting QDs to $[\text{Co}(\text{ClMeN}_3\text{S}_3\text{sar})]^{3/2+}$ has the largest driving force of the three complexes, the reason for the high rates is more because of the very low internal reorganization energy which completely changes the shape of the curve (Figure 2). In turn, the $[\text{Co}(\text{sep})]^{3/2+}$ should be faster than the $[\text{Co}(\text{en})_3]^{3/2+}$ again, not due to the driving force, which is smaller for the $[\text{Co}(\text{sep})]^{3/2+}$, but rather because of the smaller reorganization energy of the caged $[\text{Co}(\text{sep})]^{3/2+}$ compared to $[\text{Co}(\text{en})_3]^{3/2+}$.

Charge transfer from the conduction band of idealized red and green emitting CdSe QDs to $[\text{Co}(\text{sep})]^{3/2+}$ and $[\text{Co}(\text{en})_3]^{3/2+}$ are in the Marcus normal regime. In contrast, because $[\text{Co}(\text{ClMeN}_3\text{S}_3\text{sar})]^{3/2+}$ has such a low reorganization energy, the driving force is comparable in energy. As a consequence, electron transfer from red QDs to $[\text{Co}(\text{ClMeN}_3\text{S}_3\text{sar})]^{3/2+}$ is in the normal regime, but is very close to the barrierless, and even slightly into the inverted regime for the green.

The effects of the reorganization energy of the acceptor on the kinetics of charge or electron transfer were characterized by titrating solutions of red and green emitting cadmium chalcogenide QDs with these different cobalt complexes. The quantum dot fluorescence and subsequent quenches were monitored (Figure 3).

For both colors of dots, the $[\text{Co}(\text{ClMeN}_3\text{S}_3\text{sar})]^{3/2+}$ caused the most intense quenching of the three complexes. It is favored to have the fastest charge transfer of the three complexes due to its largest electrochemical driving force and minimal reorganization energy. Stern–Volmer plots were generated and their linear trends suggest either dynamic or static quenching, but not a transition between

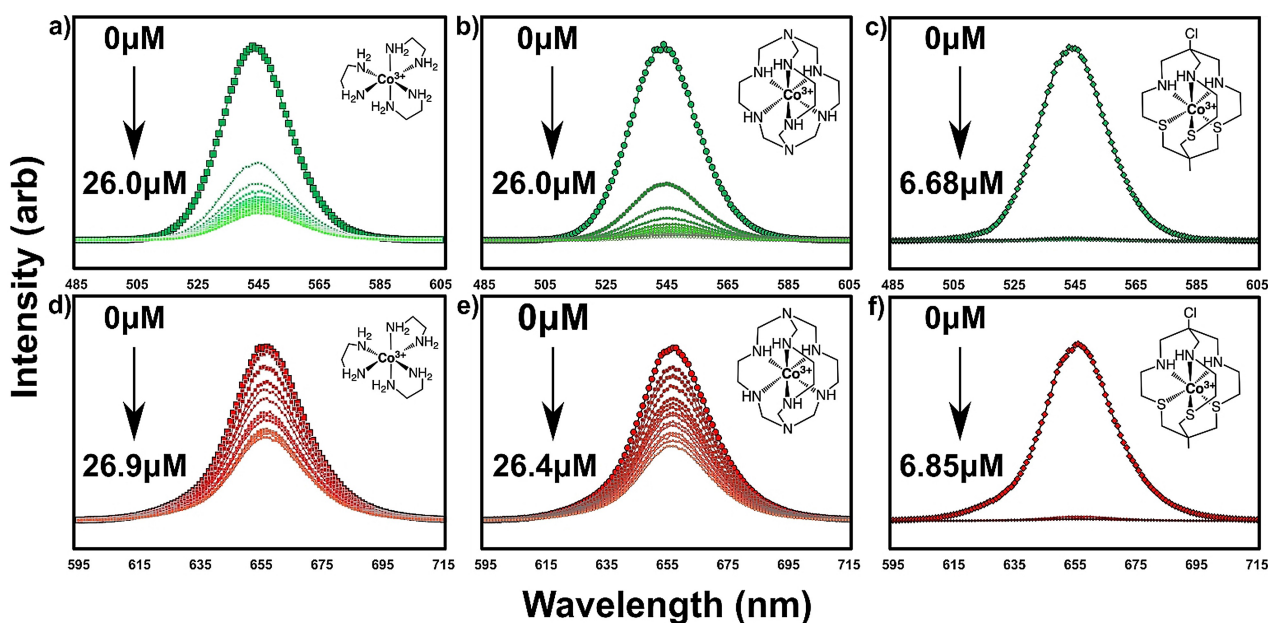


Figure 3. Steady-state fluorescence measurements of green 545 nm (a)–(c) and red 655 nm (d)–(f) emitting fluorescent QDs in the presence of cobalt complex ions a) $[\text{Co}(\text{en})_3]^{3/2+}$ (0–26.0 μM) b) $[\text{Co}(\text{sep})]^{3/2+}$ (0–26.0 μM) c) $[\text{Co}(\text{ClMeN}_3\text{S}_3\text{sar})]^{3/2+}$ (0–6.68 μM) d) $[\text{Co}(\text{en})_3]^{3/2+}$ (0–26.9 μM) e) $[\text{Co}(\text{sep})]^{3/2+}$ (0–26.4 μM) f) $[\text{Co}(\text{ClMeN}_3\text{S}_3\text{sar})]^{3/2+}$ (0–6.85 μM)

the two (Figure 4). We assume all three complexes undergo the same type of quenching. The slopes provide a more quantitative analysis of the fluorescence quench. $[\text{Co}(\text{ClMeN}_3\text{S}_3\text{sar})]^{3/2+}$ quenched the green emitting CdSe QDs ≈ 10 times more strongly than $[\text{Co}(\text{sep})]^{3/2+}$ and ≈ 60 times more than $[\text{Co}(\text{en})_3]^{3/2+}$ (Figure 4a inset). $[\text{Co}(\text{ClMeN}_3\text{S}_3\text{sar})]^{3/2+}$ quenched the red emitting CdSe@CdS QDs ≈ 260 times more strongly than $[\text{Co}(\text{sep})]^{3/2+}$ and ≈ 338 times more than $[\text{Co}(\text{en})_3]^{3/2+}$ (Figure 4b inset).

The comparison of $[\text{Co}(\text{sep})]^{3/2+}$ vs. $[\text{Co}(\text{en})_3]^{3/2+}$ highlights the importance of reorganization energy in electron transfer rates and how it can actually dominate over other trends. The driving force for charge transfer favors the $[\text{Co}(\text{en})_3]^{3/2+}$ by 0.24 V to be faster, and yet $[\text{Co}(\text{sep})]^{3/2+}$ has a much higher quench rate than $[\text{Co}(\text{en})_3]^{3/2+}$ by a factor of ≈ 6.3 for the green dots (Figure 4a) and by ≈ 1.3 for the red dots. $[\text{Co}(\text{sep})]^{3/2+}$ has a much smaller reorganization energy barrier than $[\text{Co}(\text{en})_3]^{3/2+}$ by 1.95 V. It is the reorganization energy barrier that explains the quenching rates rather than driving force in this experiment.

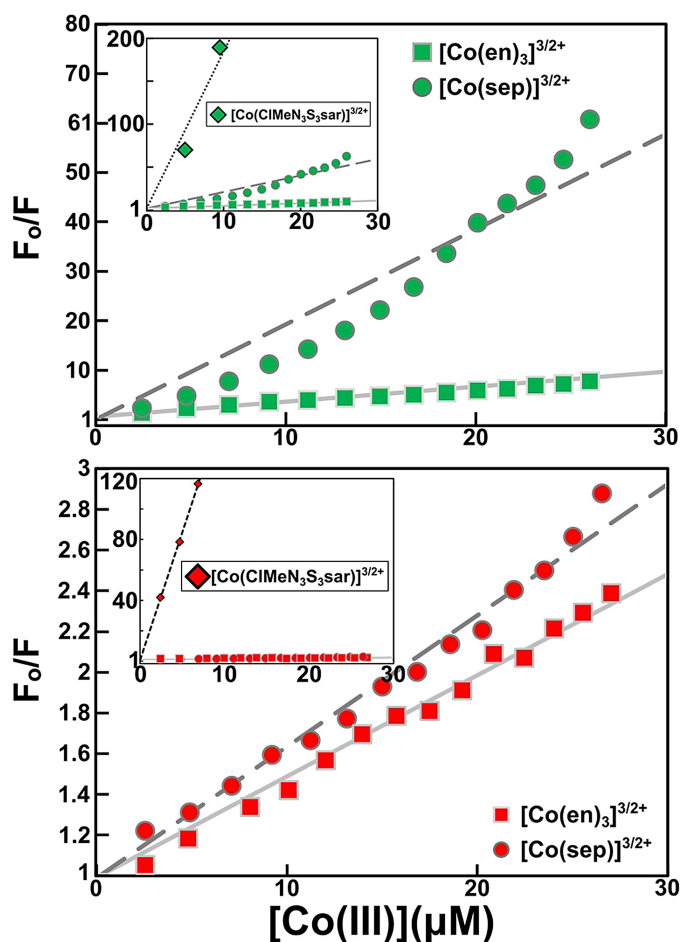


Figure 4. Stern–Volmer plots of fluorescence where F_0 is the initial summed fluorescence and F is the fluorescence in the presence of the indicated concentration of Co. a) QDs emitting at 545 nm; b) QDs emitting at 655 nm. Insets are on a higher scale and include $[\text{Co}(\text{ClMeN}_3\text{S}_3\text{sar})]^{3/2+}$.

The experimental quenching trends (Figure 4) match the trends seen in the calculated rates (Figure 2), yet closer inspection shows the experiments the $[\text{Co}(\text{en})_3]^{3/2+}$ outperforming prediction when comparing complexes in sheer orders of magnitude. Parasitic absorption by the cobalt complexes was ruled out, as it was minimal (ϵ (400 nm, $\text{M}^{-1}\text{cm}^{-1}$) $[\text{Co}(\text{en})_3]^{3/2+} = 25.5$ $[\text{Co}(\text{sep})]^{3/2+} = 14.1$, $[\text{Co}(\text{ClMeN}_3\text{S}_3\text{sar})]^{3/2+} = 391$, QDs $\approx 10^5$)²³ (Supporting Information). The most likely source of error is the assumption that the orbital overlap H_{DA} with the QD and all three complexes is the same. Secondly, the experiments also capture any other non-Marcus quenching processes and intermediate steps (such as charge transfer to a surface state) that may complicate direct comparison to the Marcus predictions.

We considered the possibility that Förster Resonant Energy Transfer (FRET) was a secondary non-radiative route for energy transfer that could complicate the interpretation for charge transfer. FRET and other resonant transfer mechanisms are dependent upon the degree of spectral overlap between the donor (QD) and the acceptor (Co^{3+}) as well as the distance between them. Using the experimental fluorescence spectra of the QDs and the absorbance spectra of the cobalt complexes, the overlap was calculated to be minimal, with the largest value of $\approx 1 \times 10^{12} \text{ J mol}^{-1} \text{ cm}^{-1} \text{ nm}^4$ for the green dots with the cobalt complexes. The spectral overlap is then used in calculating the distance under which FRET is likely, R_0 . This calculation takes into account the quantum yield of the donor QDs ($\approx 85\%$) and the $(1/d)^6$ distance dependence of the FRET process. It was determined that the R_0 for this system between 1.6 and 2.6 nm. Since the green 545 nm emitting QDs have the highest amount of overlap but also an organic shell greater than 2.5 nm (Supporting Information), FRET processes are likely very minimal in these experiments.

Nanosecond lifetime fluorescence measurements were taken of the QDs with increasing concentrations of the cobalt complexes (Figure 5) and were each fit with a tri-exponential decay function (Supporting Information). For both of the QDs measured without cobalt, each of the three decay components were matched to likely excitonic pathways according to previous literature precedent. The fastest component, ≈ 3 ns, is typically attributed to exciton carrier trapping at defects in the core of the material. The slowest component, ≈ 60 ns, is attributed to carrier trapping at nanocrystal surface defects. The intermediate-length component is attributed to direct, band edge, radiative recombination of the exciton. The green dots have a faster band edge radiative lifetime of ≈ 20 ns than that of the red dots at ≈ 27 ns, which is due to the greater overlap between the hole and electron wave functions for the smaller, green emitting QDs. Overall, the average lifetime for the green QDs was faster than the red QDs, with 19.8 ns and 36.8 ns, respectively.

The addition of the cobalt complexes in all cases decreased the average lifetimes, suggesting that the charge transfer is comparable or faster than the average lifetimes of the QDs (Figure 6). The trends in the change in average lifetime follow the predicted trends from Marcus theory when reorganization energy is considered. The effect of the

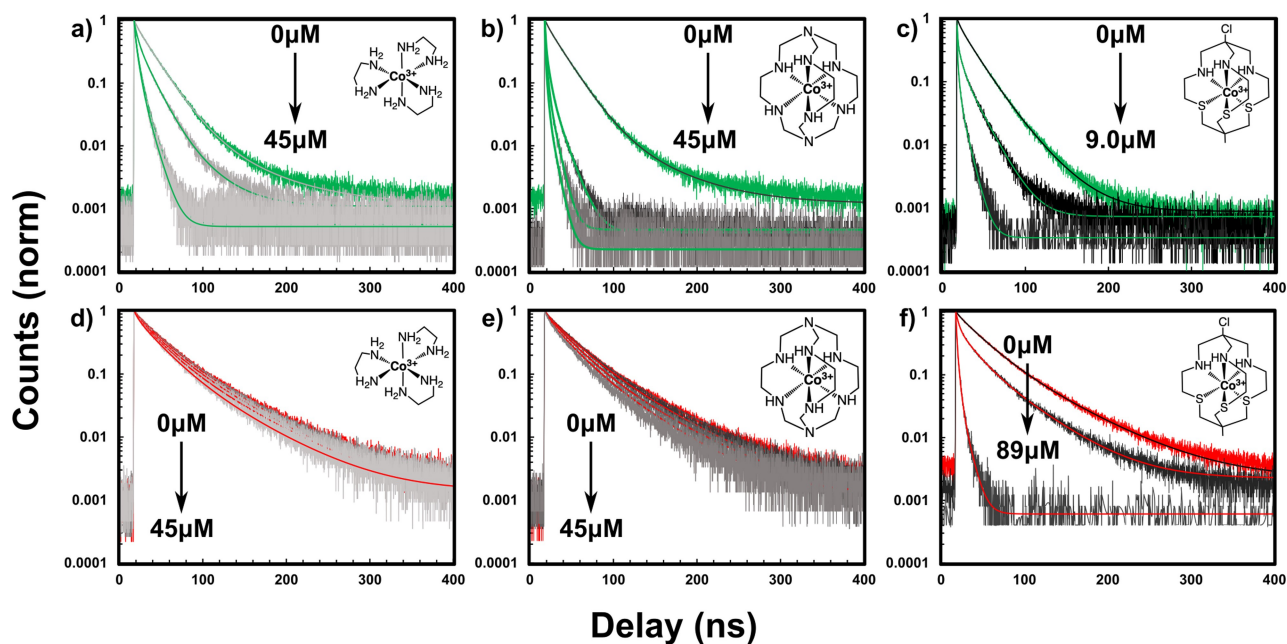


Figure 5. Time-resolved photoluminescence analysis of (top) green emitting (545 nm) and (bottom) red emitting (655 nm) CdSe QDs in the presence of a) $[\text{Co}(\text{en})_3]^{3/2+}$ (0–45 μM) b) $[\text{Co}(\text{sep})]^{3/2+}$ (0–45 μM) c) $[\text{Co}(\text{ClMeN}_3\text{S}_3\text{sar})]^{3/2+}$ (0–9.0 μM) d) $[\text{Co}(\text{en})_3]^{3/2+}$ (0–45 μM) e) $[\text{Co}(\text{sep})]^{3/2+}$ (0–45 μM) f) $[\text{Co}(\text{ClMeN}_3\text{S}_3\text{sar})]^{3/2+}$ (0–98 μM).

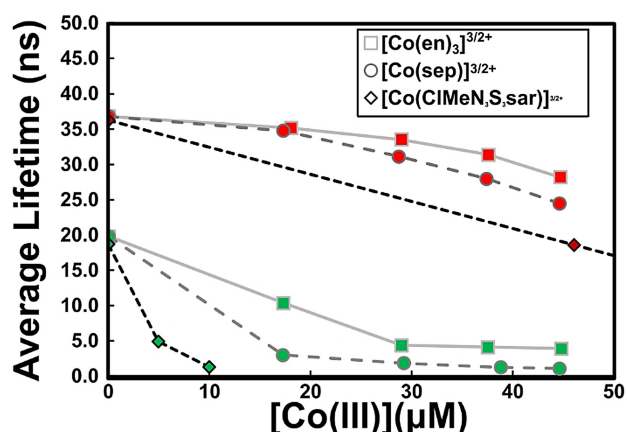


Figure 6. Average fluorescence lifetimes of green and red emitting CdSe QDs (markers colored accordingly) in the presence of three cobalt complex ions at varying concentrations.

reorganization energy is far more pronounced for the green QDs over the red QDs due to the larger driving force for electron transfer from the raised QD conduction band to the cobalt complexes. For both red and green emitting QDs, the addition of $[\text{Co}(\text{en})_3]^{3/2+}$ decreased the average lifetime, but the effect was greater for $[\text{Co}(\text{sep})]^{3/2+}$ and even more so for $[\text{Co}(\text{ClMeN}_3\text{S}_3\text{sar})]^{3/2+}$. The near vertical decays seen at short times for the $[\text{Co}(\text{ClMeN}_3\text{S}_3\text{sar})]^{3/2+}$ with the green and red dots and the $[\text{Co}(\text{sep})]^{3/2+}$ with the green dots suggests that the lifetimes were so short that they exceeded the capabilities of the instrumentation. These observations match the calculated prediction that $[\text{Co}(\text{en})_3]^{3/2+}$ should have the slowest charge transfer.

Once the time-resolved fluorescence curves were fitted with tri-exponentials (Supporting Information), some more information about approximate charge transfer rates could be identified that matched the predicted trends. In the combinations where the charge transfer rates were expected to be the highest— $[\text{Co}(\text{ClMeN}_3\text{S}_3\text{sar})]^{3/2+}$ with red or green QDs, and $[\text{Co}(\text{sep})]^{3/2+}$ with green dots—the time-resolved fluorescence saw the emergence of a new, extremely short component, that was fitted to be sub-nanosecond. For the combinations with the slowest predicted rates,— $[\text{Co}(\text{en})_3]^{3/2+}$ with green or red QDs and $[\text{Co}(\text{sep})]^{3/2+}$ with red QDs—the fittings showed increased contributions from components between 1–5 ns. One interpretation of this result is that charge transfer occurs at this time scale for these combinations. Due to limitations of the detector, it is not possible to fit these the sub-nanosecond lifetimes with any greater detail, however the results agree with the predicted trends by Marcus theory. Spectroscopies that have picosecond resolution such as transient absorption are planned to achieve exact values of k_{ET} .

The ratio of the rates for electron transfer for the green vs the red dots illustrates that Marcus theory, while useful, is yet incomplete in describing this system. In general, once normalized for the difference in tunnelling barriers between the red and green QDs (approximated in Supporting Information), we expect that of the three complexes, charge transfer rates to $[\text{Co}(\text{ClMeN}_3\text{S}_3\text{sar})]^{3/2+}$ to show the smallest improvement upon increasing driving force from red to green QDs; while charge transfer from green QDs to $[\text{Co}(\text{ClMeN}_3\text{S}_3\text{sar})]^{3/2+}$ is in the Marcus inverted regime and should be moderated. However, experimentally, we observed that the improvement upon increasing the driving

force for charge transfer to $[\text{Co}(\text{ClMeN}_3\text{S}_3\text{sar})]^{3/2+}$ greatly outpaced the other two complexes. We attribute this difference to Auger-Assisted Charge transfer, which is most impactful at the barrierless and inverted regimes, and therefore is most effective in charge transfer from green dots to $[\text{Co}(\text{ClMeN}_3\text{S}_3\text{sar})]^{3/2+}$ (Figure 2). As the other combinations of QDs and complexes are far below the barrierless or inverted regimes, the effects of Auger-Assisted Charge transfer are modest.

Conclusion

A series of Co-based redox mediators with varying reorganization energies and similar electrochemical potentials were studied for their charge transfer from QDs. Marcus theory predicts that both driving force to the acceptor and the reorganization energy effect charge transfer rates. In this case, the theory predicted that the effect of minimizing reorganization energy would far outweigh the subtler effect of varying driving force on maximizing the charge transfer rates.

The N/S mixed donor redox mediator $[\text{Co}(\text{ClMeN}_3\text{S}_3\text{sar})]^{3/2+}$, has the smallest internal reorganization energy of the three cobalt complexes at only 0.83 eV. This compound has a cage structure that prevents ligand movement, and belongs to a select family of ions where both the Co^{II} and Co^{III} species are low spin due to the influence of the S-donor atoms, which requires very little movement in the ligand shell to support changing oxidation state. These features allow it to have a smaller reorganization energy than the rigidly caged $[\text{Co}(\text{sep})]^{3/2+}$ ($\lambda=1.82$ eV) and the relatively floppy $[\text{Co}(\text{en})_3]^{3/2+}$ ($\lambda=2.79$ eV).

In steady-state quenching experiments low reorganization energy $[\text{Co}(\text{ClMeN}_3\text{S}_3\text{sar})]^{3/2+}$ was able to quench green and red QDs 140 and 180 times more effectively than $[\text{Co}(\text{en})_3]^{3/2+}$, respectively. Time-resolved photoluminescence experiments suggests that the charge transfer to $[\text{Co}(\text{en})_3]^{3/2+}$ was 1–5 ns, but transfer to $[\text{Co}(\text{sep})]^{3/2+}$ (with a large driving force) or $[\text{Co}(\text{ClMeN}_3\text{S}_3\text{sar})]^{3/2+}$ was even faster than the instrument could measure and could only be deemed as sub-nanosecond.

Comparison of the predicted rates and the average rates observed by TRPL suggest that Auger-Assisted electron transfer is an active mechanism for charge transfer that was not predicted by the Marcus Model employed.

Previous studies of charge transfer from QDs to charge acceptors, are often performed in organic solvents, which serendipitously lower solvent reorganization energy. However, many applications of QDs, such as photocatalytic water splitting and biological applications require solvation in water. Here, we chose to study charge transfer kinetics under these more stringent conditions, to ensure that the results were relevant to applications.

The results here suggest that careful design of the ligand environment of redox mediators to reduce reorganization energy is an important route forward in improving technologies where charge transfer from QDs is featured.

Acknowledgements

Funding Sources: J.E.M. and M.J.F. are thankful for funding provided by the U.S. National Science Foundation TNSCORE NSF EPS 1004083 and the Vanderbilt Institute for Nanoscale Science and Engineering. S.M.C. and S.J.R. thank U.S. National Science Foundation CHE 1506587. M.J.F. and S.M.C. thank the Vanderbilt Institute of Nanoscale Science and Engineering Graduate Fellowship. P.V.B. thanks the Australian Research Council Discovery Project DP190103158.

Conflict of Interest

The authors declare no conflict of interest.

Data Availability Statement

The data that support the findings of this study are available in the Supporting Information of this article.

Keywords: Charge Transfer · Cobalt Cage Complexes · Metal Cage Complexes · Quantum Dots · Time-Resolved Photoluminescence

- [1] M. V. Kovalenko, L. Manna, A. Cabot, Z. Hens, D. V. Talapin, C. R. Kagan, V. I. Klimov, A. L. Rogach, P. Reiss, D. J. Milliron, P. Guyot-Sionnest, G. Konstantatos, W. J. Parak, T. Hyeon, B. A. Korgel, C. B. Murray, W. Heiss, *ACS Nano* **2015**, *9*, 1012–1057.
- [2] Z. Han, F. Qiu, R. Eisenberg, P. L. Holland, T. D. Krauss, *Science* **2012**, *338*, 1321–1324.
- [3] R. C. Somers, M. G. Bawendi, D. G. Nocera, *Chem. Soc. Rev.* **2007**, *36*, 579–591.
- [4] P. T. Snee, R. C. Somers, G. Nair, J. P. Zimmer, M. G. Bawendi, D. G. Nocera, *J. Am. Chem. Soc.* **2006**, *128*, 13320–13321.
- [5] R. D. Harris, S. Bettis Homan, M. Kodaimati, C. He, A. B. Nepomnyashchii, N. K. Swenson, S. Lian, R. Calzada, E. A. Weiss, *Chem. Rev.* **2016**, *116*, 12865–12919.
- [6] N. Hildebrandt, C. M. Spillmann, W. Russ Algar, T. Pons, M. H. Stewart, E. Oh, K. Susumu, S. A. Díaz, J. B. Delehanty, I. L. Medintz, *Chem. Rev.* **2017**, *117*, 536–711.
- [7] J. Owen, L. Brus, *J. Am. Chem. Soc.* **2017**, *139*, 10939–10943.
- [8] B. Y. Xia, P. Yang, Y. Sun, Y. Wu, B. Mayers, B. Gates, Y. Yin, F. Kim, H. Yan, *Adv. Mater.* **2003**, *15*, 353–389.
- [9] M. B. Wilker, K. J. Schnitzenbaumer, G. Dukovic, *Isr. J. Chem.* **2012**, *52*, 1002–1015.
- [10] N. J. Orfield, J. R. McBride, F. Wang, M. R. Buck, J. D. Keene, K. R. Reid, H. Htoon, J. A. Hollingsworth, S. J. Rosenthal, *ACS Nano* **2016**, *10*, 1960–1968.
- [11] N. J. Orfield, S. Majumder, J. R. McBride, F. Yik-Ching Koh, A. Singh, S. J. Bouquin, J. L. Casson, A. D. Johnson, L. Sun, X. Li, C. K. Shih, S. J. Rosenthal, J. A. Hollingsworth, H. Htoon, *ACS Nano* **2018**, *12*, 4206–4217.
- [12] J. H. Olshansky, T. X. Ding, Y. V. Lee, S. R. Leone, A. P. Alivisatos, *J. Am. Chem. Soc.* **2015**, *137*, 15567–15575.
- [13] T. X. Ding, J. H. Olshansky, S. R. Leone, A. P. Alivisatos, *J. Am. Chem. Soc.* **2015**, *137*, 2021–2029.

- [14] R. A. Marcus, N. Sutin, *Biochim. Biophys. Acta Rev. Bioenerg.* **1985**, *811*, 265–322.
- [15] R. A. Marcus, *Angew. Chem. Int. Ed. Engl.* **1993**, *32*, 1111–1121; *Angew. Chem.* **1993**, *105*, 1161–1172.
- [16] F. M. C. He, P. V. Bernhardt, *J. Biol. Inorg. Chem.* **2017**, *22*, 775–788.
- [17] K. B. Ørnsø, E. O. Jónsson, K. W. Jacobsen, K. S. Thygesen, *J. Phys. Chem. C* **2015**, *119*, 12792–12800.
- [18] S. A. Sapp, C. M. Elliott, C. Contado, S. Caramori, C. A. Bignozzi, *J. Am. Chem. Soc.* **2002**, *124*, 11215–11222.
- [19] K. Han, M. Wang, S. Zhang, S. Wu, Y. Yang, L. Sun, *Chem. Commun.* **2015**, *51*, 7008–7011.
- [20] C. Gimbert-Suriñach, J. Albero, T. Stoll, J. Fortage, M. N. Collomb, A. Deronzier, E. Palomares, A. Llobet, *J. Am. Chem. Soc.* **2014**, *136*, 7655–7661.
- [21] W. T. Eckenhoff, W. R. McNamara, P. Du, R. Eisenberg, *Biochim. Biophys. Acta Bioenerg.* **2013**, *1827*, 958–973.
- [22] P. V. Bernhardt, L. A. Jones, *Inorg. Chem.* **1999**, *38*, 5086–5090.
- [23] W. W. Yu, L. Qu, W. Guo, X. Peng, *Chem. Mater.* **2003**, *15*, 2854–2860.
- [24] S. M. Feldt, G. Wang, G. Boschloo, A. Hagfeldt, *J. Phys. Chem. C* **2011**, *115*, 21500–21507.
- [25] A. Yella, H.-W. Lee, H. N. Tsao, C. Yi, A. K. Chindrian, M. K. Nazeeruddin, E. W.-G. Diau, C.-Y. Yeh, *Science* **2011**, *334*, 629–633.
- [26] Y. Xie, T. W. Hamann, *J. Phys. Chem. Lett.* **2013**, *4*, 328–332.
- [27] M. K. Kashif, M. Nippe, N. W. Duffy, C. M. Forsyth, C. J. Chang, J. R. Long, L. Spiccia, U. Bach, *Angew. Chem. Int. Ed.* **2013**, *52*, 5527–5531; *Angew. Chem.* **2013**, *125*, 5637–5641.
- [28] R. V. Dubs, L. R. Gahan, A. M. Sargeson, *Inorg. Chem.* **1983**, *22*, 2523–2527.
- [29] W. A. Tisdale, X. Y. Zhu, *Proc. Natl. Acad. Sci. USA* **2011**, *108*, 965–970.
- [30] H. Zhao, Y. Li, L. Diau, C. Sun, Y. Shi, *Spectrochim. Acta Part A* **2019**, *218*, 237–242.
- [31] M. Chou, C. Creutz, N. Sutin, *J. Am. Chem. Soc.* **1977**, *99*, 5615–5623.
- [32] I. I. Creaser, A. M. Sargeson, A. W. Zanella, *Inorg. Chem.* **1983**, *22*, 4022–4029.
- [33] L. R. Gahan, J. M. Harrowfield, *Polyhedron* **2015**, *94*, 1–51.
- [34] P. Osvath, A. M. Sargeson, A. McAuley, R. E. Mendelez, S. Subramanian, M. J. Zaworotko, L. Broge, *Inorg. Chem.* **1999**, *38*, 3634–3643.
- [35] A. W. H. Mau, W. H. F. Sasse, A. M. Sargeson, *Aust. J. Chem.* **1993**, *46*, 641–661.
- [36] P. Osvath, A. M. Sargeson, B. W. Skelton, A. H. White, *J. Chem. Soc. Chem. Commun.* **1991**, 1036–1038.
- [37] R. G. Endres, M. X. LaBute, D. L. Cox, *J. Chem. Phys.* **2003**, *118*, 8706–8714.
- [38] T. J. Zerk, C. T. Saouma, J. M. Mayer, W. B. Tolman, *Inorg. Chem.* **2019**, *58*, 14151–14158.
- [39] H. Zhu, Y. Yang, K. Hyeon-Deuk, M. Califano, N. Song, Y. Wang, W. Zhang, O. V. Prezhdo, T. Lian, *Nano Lett.* **2014**, *14*, 1263–1269.

Manuscript received: February 11, 2022

Accepted manuscript online: April 27, 2022

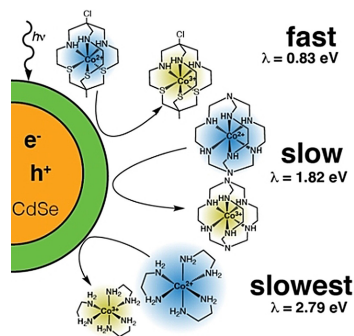
Version of record online: ■■■, ■■■

Research Articles

Quantum Dots

M. J. Fort, S. M. Click, E. H. Robinson,
F. M. C. He, P. V. Bernhardt, S. J. Rosenthal,
J. E. Macdonald* [e202202322](#)

Minimizing the Reorganization Energy of
Cobalt Redox Mediators Maximizes Charge
Transfer Rates from Quantum Dots



Choosing a redox-mediator with low reorganization energy vastly improves charge transfer rates from quantum dots by orders of magnitude.